Mammalian Genome 10, 88–94 (1999).

Mammalian Genome
Incorporating Mouse Genome

Mapping and cloning recombinant breakpoints demarcating the Hybrid Sterility 6-specific sperm tail assembly defect

Sadhara A. Samant,[1] John Fossella,[2] Lee M. Silver,[2] Stephen H. Pilder[1]

[1]Department of Anatomy and Cell Biology, Temple University School of Medicine, 3400 North Broad Street, Philadelphia, Pennsylvania 19140, USA
[2]Department of Molecular Biology, Princeton University, Washington Road, Princeton, New Jersey 08540, USA

Received: 12 August 1998 / Accepted: 1 October 1998

Abstract. Variants of the mouse *t* complex known as *t* haplotypes *(t)* express factors that perturb sperm differentiation, resulting in the non-Mendelian transmission of *t* from +/*t* heterozygous males and the sterility of *t*/*t* homozygous males. Previous studies of mice carrying heterospecific combinations of the *t* complex have revealed a 1-cM candidate locus, *Hst6,* for the distal-most of these factors, *Tcd/Tcs2.* Males heterozygous for the *M. spretus* allele of *Hst6* and a *t* haplotype (*Hst6*^{s}/*t*) are sterile, expressing an abnormality in sperm flagellar curvature (''curlicue'') indistinguishable from one exhibited by sperm from *t*/*t* homozygotes. *Hst6*^{s}/*Hst6*^{s} males are also sterile; however, sperm produced by these males are completely immotile owing to the absence of assembled flagella. Recent studies have shown that the complete presentation of ''curlicue'' derives from expression of at least two factors within the locus, Curlicue a (*Ccua*) proximally and Curlicue b (*Ccub*) distally, with a factor affecting sperm-oolemma penetration, *Stop1p,* mapping between them. In the present report, we have examined expression of the *Hst6*-specific flagellar assembly phenotype in sperm from mice homozygous for *M. spretus–M. m. domesticus* recombinant Chr 17 homologs whose breakpoints map within the *Hst6* locus. SSLP analysis of these homologs has demonstrated that the flagellar assembly defect maps to less than 0.2 cM between *D17Mit61* and *D17Mit135,* coincident with *Ccua.* SSR content analysis of 23 BACs mapping to four contigs within the *Hst6* locus has resulted in isolation of proximal and distal recombinant breakpoints circumscribing the flagellar assembly phenotype/*Ccua* factor. In addition, we have provided increased high-resolution mapping of the *Stop1p* and *Ccub* factors. These new data enhance our ability to isolate and characterize candidates for *Tcd/Tcs2.*

Introduction

The proximal third of mouse Chr 17, known as the *t* complex, is found in two alternative forms in natural populations of the house mouse, *M. musculus,* and its various subspecies. The major form is designated wildtype (+), while a more minor form, called a *t* haplotype (*t*), is detected at a relatively lower equilibrium frequency (Fig. 1). These two forms of the *t* complex are distinguished from each other first, by major structural variations, and second, by their differential effects on sperm function.

In +/*t* heterozygotes, recombination is suppressed nearly completely because all *t* haplotypes contain four large, non-overlapping inversions (*In(17)1–In(17)4*) that span about 90% of the *t* complex region relative to + homologs (Fig. 1; Hammer et al. 1989). Within the confines of three of the large *t*-inversions are housed several genetically interacting factors that negatively affect the transmission ratio of +-bearing sperm produced by +/*t* heterozygotes, and cause the complete sterility of *t*-homozygous males (Lyon 1984, 1986). These elements have been called *t* complex distorter (*Tcd*) or *t* complex sterility (*Tcs*) factors, depending on whether the respective phenotype is one of +/*t* transmission ratio distortion (TRD) or *t*/*t* male sterility (Fig. 1). Isolation of these elements has proved difficult because +/*t* recombination suppression has hindered their high-resolution mapping.

In recent breeding studies, introgression of a Chr 17 homolog (*S*; Fig. 1) from the aboriginal mouse species *Mus spretus* into the *Mus musculus domesticus* genetic background revealed a singular *S/t* phenotype of male sterility (Hammer et al. 1989). Because *S* and + homologs were not inverted relative to each other in the *t* inversions housing *Tcd/Tcs* factors, it was possible to produce intra-inversion *S*-+ recombinant Chr 17 homologs that could be employed as indirect mapping tools for the high-resolution localization of *t* haplotype-specific sterility factors and, thus, *Tcd/Tcs* candidates. In total, four loci, Hybrid Sterility 4, 5, 6, and 7 (*Hst4–7*) were found to contribute to this unique *S/t* phenotype of male sterility (Fig. 1; Pilder et al. 1991, 1993, 1997; Pilder 1997). *Hst4–6* mapped to the largest and most distal of the inversions, *In(17)4,* coincident with the strongest of the *Tcd/Tcs* factors, *Tcd/Tcs2,* while *Hst7* mapped to the smallest and most proximal inversion, *In(17)1,* coincident with a weaker *Tcd/Tcs* factor, *Tcd/Tcs1.*

One of the more interesting *Hst* elements is *Hst6,* mapping to a 1-cM region within the 10-cM *In(17)4* (Fig. 1). Males heterozygous for the *Mus spretus* allele of *Hst6* and a *t* haplotype (*Hst6*^{s}/*t*) are completely sterile. In addition, these animals produce sperm exhibiting a *t*-homozygous-specific defect in flagellar curvature known as ''curlicue'', in which the flagella of motile sperm form a spiral shaped curl that bends in the direction opposite to the curvature of the sperm head (Pilder et al. 1993; Olds-Clarke and Johnson 1993). Interestingly, *Hst6*^{s} homozygous males are also completely sterile. However, sperm produced by these males are completely immotile, owing to the absence of assembled flagella (Pilder et al. 1993; Phillips et al. 1993). Initial data have suggested that a single gene model is sufficient to account for both the ''curlicue'' phenotype and ''unassembled flagellum'' phenotype, hereafter referred to as the ''whipless'' phenotype. In this model, the *s* allele of *Hst6* is a recessive loss-of-function allele affecting flagellar assembly, while the *t* allele is an altered-function allele affecting flagellar function. Thus, if this model is correct, an *Hst6*^{s}/*Hst6*^{t} male is functionally hemizygous for the *Hst6*^{t} allele, and therefore expresses the *t*-homozygous ''curlicue'' phenotype (Pilder et al. 1993).

Recently, we presented quantitative evidence that strongly suggested that the ''curlicue'' phenotype is the product of more than one gene, a Curlicue a (*Ccua*) gene in the proximal portion of the *Hst6* locus, and a Curlicue b (*Ccub*) gene mapping to the distal portion of the *Hst6* locus (Redkar et al. 1998). In the same work, data were also presented strongly suggesting the existence of a

Correspondence to: S.H. Pilder

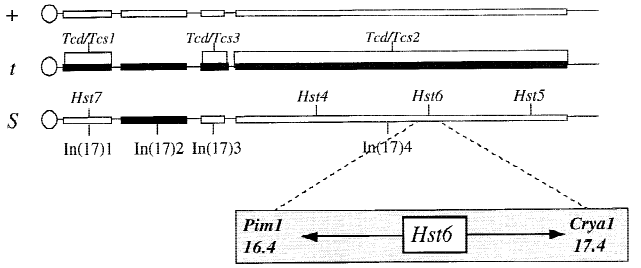

Fig. 1. Diagram of three *t* complex homologs (not drawn precisely to scale). The top line represents the *M. m. domesticus* wildtype (+) homolog, the middle line, the *t* haplotype (*t*) homolog, and the bottom line, the *M. spretus* (*S*) homolog. The abbreviation for each homolog is to the left of that homolog's centromere, represented by a circle. Boxed regions represent the *t*-associated inversions, *In(17)1-In(17)4*, shown below the *S* homolog. Differences in color of the boxes illustrate the orientation of the inversions in one homolog relative to the orientation in the other homologs. The *t*-specific, genetically interacting male distorter/sterility factors, *Tcd/Tcs1, Tcd/Tcs2,* and *Tcd/Tcs3* are shown above the inversions of the *t* haplotype homolog to which they map, and the brackets extending below the *Tcd/Tcs* factor abbreviations show the gross intra-inversion map positions of these factors. The approximate map positions of *Hst4, 5, 6,* and *7* are shown above the representation of the *S* homolog. The ~ 1 cM *Hst6* locus is shown in enlargement at the bottom of the figure with flanking markers *Pim1* and *Crya1*.

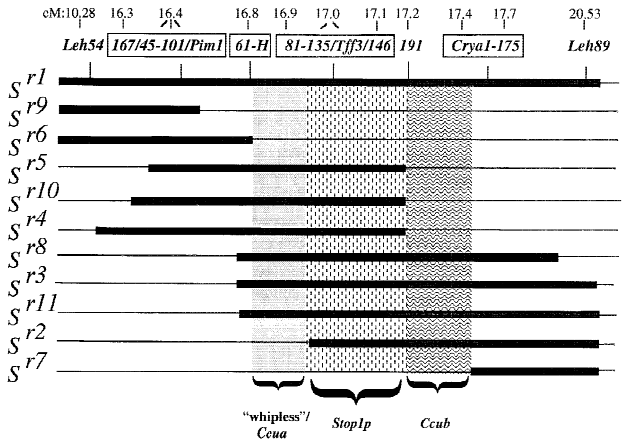

Fig. 2. An aggregate genetic/partial physical map of *Hst6.* The 11 *S*-+ recombinant Chr 17 homologs used in this study are drawn as horizontal lines. Black boxes represent *S* chromatin, while thin horizontal lines represent + chromatin. The names of homologs are denoted to the left of each line. DNA markers used to type each recombinant homolog are indicated above the diagram of S^{r1} and are described in Materials and methods. The abbreviations *Leh54* and *Leh89* stand for *D17Leh54* and *D17Leh89,* and represent markers at the proximal and distal ends of the wildtype form of the *In(17)4,* respectively. The abbreviations *167* through *175* from proximal to distal represent the *D17Mit167* through *D17Mit175* SSRs (MAPPAIRS purchased from Research Genetics), and *H* is an abbreviation for the marker *H6.7b.* Boxed markers are those found in the same BAC contig. Hyphens between adjacent boxed markers mean that those markers have been found on the same BAC clone(s), and slashes between adjacent boxed markers mean that those markers have been found on different BAC clones. Shown above the DNA marker designations are their approximate genetic map positions in centiMorgans (cM). The three rectangular shaded areas central to the figure represent from left to right the map positions of the ''whipless''/*Ccua* (grey rectangle), *Stop1p* (vertically dashed rectangle), and *Ccub* (wavily lined rectangle) loci, respectively, with respect to both genotypic and phenotypic analyses.

gene, *Stop1p,* affecting the ability of sperm to penetrate the zona pellucida-free oocyte in vitro, mapping between the *Ccua* and *Ccub* genes. Here we report the cloning of *S*-+ recombinant breakpoints that delimit the portion of the *Hst6* locus corresponding to the expression of the ''whipless'' phenotype. We show that this region is less than 0.2 cM in size, mapping distal to 16.8 and proximal to 17.0 cM on the Chr 17 map, and coinciding with the map position of the *Ccua* locus. In addition, we more precisely define the map positions of the *Stop1p* and *Ccub* genes.

Materials and methods

Experimental animals and Chr 17 genotyping. All animals used in these experiments were bred and maintained in the colony of S. Pilder, and carried either the C57BL/6 or 129/Sv^{+c+p} genetic background. The breeding strategy used to produce test animals carrying various *S*-+ recombinant Chr 17 genotypes has been described (Pilder et al. 1993). Recombinant Chr 17 homologs were defined according to the alleles present at the marker loci: *D17Leh54, Hbaps4, Pim1, Crya1, D17Leh89, D17Mit61, D17Mit81, D17Mit135, D17Mit146, D17Mit191* (Hamvas et al. 1998), and novel DNA polymorphisms mapping to the proximal half of the *Pim1* to *Crya1* interval formerly referred to as *Spretus-Hst6p* sequences (Redkar et al. 1998). Genomic DNAs were extracted from mouse tail-tip biopsies (Pilder et al. 1991), and alleles were detected by either Southern blot-RFLP analysis of *Taq* I-digested genomic DNAs (Pilder et al. 1991) or by amplification of genomic DNAs under standard PCR conditions and evaluation of size polymorphisms on agarose gels (Pilder 1997). Probe DNAs for *D17Leh54, Hbaps4, Pim1, Crya1,* and *D17Leh89* have been described (Pilder et al. 1991). The probe for the *Spretus-Hst6p* sequences is a 2-kb DNA fragment isolated from subtraction assays (Fossella et al. in preparation), and is hereafter referred to as *H6.7b* in the text and *''H''* in Fig. 2. Oligonucleotide primer pairs for the *D17Mit* markers were purchased from Research Genetics (Huntsville, Ala.).

BAC isolation, DNA preparation, end sequencing, and SSR content mapping. Anchor probes for *Pim1, Crya1, Tff3* (Intestinal Trefoil Factor 3, mapping to 17.0 cM on mouse Chr 17; Hamvas et al. 1998), and *H6.7b* were used initially to screen the CITB-CJ7-B BAC library, derived from the 129/Sv mouse strain (Research Genetics). The *Tff3* probe consists of the 147-bp second exon of the gene, produced by PCR from 129/Sv genomic DNA using the forward and reverse primers 5′-ctccaagccaatgtatggtgc-3′ and 5′-tctcctgcagaggtttgaagc-3′ respectively (Chinery et al. 1996). Subsequent BAC clones were screened from the library by PCR, with primers developed from sequences of BAC ends (Table 2). PCR assays of genomic DNA isolated from the somatic cell hybrid cell lines EJ167 (containing mouse Chrs 17 and 3) and R44.1 (containing mouse Chrs 17 and 18) with BAC end primers were performed randomly to insure against BAC chimerism.

BAC DNA samples were prepared by a modified alkaline lysis technique from 250 ml bacterial cultures grown in Terrific Broth. Briefly, cleared lysates were precipitated with isopropanol, washed in 70% ethanol, resuspended in 300 μl of 10 mM Tris/1 mM EDTA, pH 8, and digested with 10 units of RNase One (Promega, Madison, WI) for 30 min at 37°C. After one extraction with phenol/chloroform, the aqueous phases were precipitated with isopropanol, washed in 70% ethanol, resuspended in 300 μl of 10 mM Tris/1 mM EDTA, pH 8, and desalted and concentrated on Microcon 50 columns (Millipore, Bedford, Mass.). BAC ends were sequenced manually by the cycle sequencing technique using ThermoSequenase and [α-^{33}P]-labeled dideoxy terminators (Amersham, Arlington Heights, Ill.). To develop BAC end primers, end sequences were analyzed with the BLAST program via the Internet.

SSR content mapping was performed by PCR with oligonucleotide primer pairs for the *D17Mit* markers listed in Table 3. Primer pairs were purchased from Research Genetics. Briefly, ~1 ng of each BAC DNA was amplified in 25 μl of a reaction mixture containing 20 pmol of each primer, 200 μM of each dNTP, 0.125 U of Taq DNA polymerase (Qiagen, Valencia, Calif.), 1× PCR buffer containing 1.5 mM $MgCl_2$ (Qiagen), and 1× Q solution (Qiagen), a PCR additive that promotes denaturation of genomic DNA. PCR assays were performed in the 9600 Thermal Cycler (Perkin Elmer, Foster City, Calif.) according to the following parameters: 94°C for 3 min + 35 cycles of 94°C for 30 s, 56°C for 30 s, and 72°C for 1 min + 72°C for 10 min. Amplified DNAs were analyzed on 3% Metaphor agarose gels (FMC, Rockville, Me.).

Sperm preparation and assessment of sperm morphology. Sperm were prepared and viewed by light microscopy as previously described

Table 1. Alleles of selected SSRs carried by S-+ recombinant Chr 17 homologs.

Homolog	''whipless''	D17Mit61	D17Mit81	D17Mit135	D17Mit146	D17Mit191
Sr1	YES	s	s	s	s	s
Sr2	NO	+	+	s	s	s
Sr3	YES	s	s	s	s	s
Sr4	YES	s	s	s	s	+
Sr5	YES	s	s	s	s	+
Sr6	NO	s	+	+	+	+
Sr7	NO	+	+	+	+	+
Sr8	YES	s	s	s	s	s
Sr9	NO	+	+	+	+	+
Sr10	YES	s	s	s	s	+
Sr11	YES	s	s	s	s	s

+: *M. musculus* allele.
s: *M. spretus* allele.

(Pilder et al. 1993, 1997; Olds-Clarke and Johnson 1993). Briefly, the caudae epididymides of each male were minced and placed in 400 μl of a modified Krebs-Ringer bicarbonate medium containing 1.7 mM calcium, and supplemented with 2% BSA (IVF medium; Neill and Olds-Clarke 1987). After 10 min incubation at 37°C in 5% CO_2 in air, epididymal tissue was removed and sperm concentration was determined by hemocytometer count. Ten min after release from the caudae, an aliquot of each sperm suspension was diluted and videotaped for 5 min at a magnification of 256× for assessment of sperm morphology.

MGD data accession number for this manuscript: J:48214.

Results

Phenotypic mapping of the ''whipless'' defect. Sperm from males homozygous for 11 different *S-+* recombinant chromosomes (S^{r1}–S^{r11}; Fig. 2; see Materials and methods for genotyping details) were tested for expression of the ''whipless'' phenotype. S^{r1} contains *M. spretus* chromatin spanning the entirely of *In(17)4* with a proximal breakpoint just proximal to the marker *D17Leh54* and a distal breakpoint just distal to *D17Leh89* (Redkar et al. 1998). The Chr 17 homologs S^{r2}–S^{r11} are all derived from the S^{r1} homolog by successive rounds of breeding and recombination. Sperm from males homozygous for S^{r2}, S^{r6}, S^{r7}, and S^{r9} do not express the ''whipless'' phenotype, while sperm from males homozygous for S^{r1}, S^{r3}, S^{r4}, S^{r5}, S^{r8}, S^{r10}, and S^{r11} do. In addition, no compound heterozygote carrying either S^{r2}, S^{r6}, S^{r7}, or S^{r9} as one of the homologs produces sperm that exhibits the ''whipless'' phenotype, while compound heterozygotes of the S^{r1}, S^{r3}, S^{r4}, S^{r5}, S^{r8}, S^{r10}, and S^{r11} homologs produce sperm expressing the ''whipless'' flagellar assembly defect. Furthermore, the ''whipless'' phenotype is nearly completely penetrant in all males expressing it, while sperm from homozygotes and compound heterozygotes not expressing this phenotype appear morphologically normal (data not shown). These data and previously published evidence showing that the S^{r2} proximal *S-+* recombinant breakpoint is more proximal than that of S^{r7} (Redkar et al. 1998) indicate that expression of the ''whipless'' defect derives from that part of the *Pim1* to *Crya1* interval bounded proximally by the S^{r6} and/or S^{r9} distal *S-+* recombinant breakpoints and distally by the S^{r2} proximal *S-+* recombinant breakpoint (Fig. 2).

SSLP mapping of recombinant Chr 17 homologs. SSLPs within the *Pim1* (16.4 cM) to *Crya1* (17.4 cM) interval have been determined by PCR for S^{r1}–S^{r11} (Table 1; Fig. 2) with oligonucleotide primers to the following subset of SSRs: *D17Mit61* (16.8 cM), *D17Mit81* (16.9 cM), *D17Mit135* (17.0 cM), *D17Mit146* (17.1 cM), and *D17Mit191* (17.2 cM). S^{r1}, S^{r3}, S^{r8}, and S^{r11} carry *M. spretus(s)* alleles of all SSRs used in this assay, while S^{r7} and S^{r9} have *M. musculus* (+) alleles at all loci. S^{r6} carries the *s* allele of *D17Mit61* and + alleles at all other loci. The recombinants S^{r4}, S^{r5}, and S^{r10} have the *s* alleles of *D17Mit61, D17Mit81, D17Mit135,* and *D17Mit146,* but the + allele of *D17Mit191.* Finally, S^{r2} carries the + alleles of *D17Mit61* and *D17Mit81,* but the *s* alleles of *D17Mit135, D17Mit146,* and *D17Mit191.* Because these data indicate that the distal recombinant breakpoint of S^{r6} is more distally located than that of S^{r9}, the distal breakpoint of S^{r6} (distal to *D17Mit61*) must define the proximal boundary of the region responsible for expression of the ''whipless'' phenotype, while the proximal breakpoint of S^{r2}, mapping between *D17Mit81* and *D17Mit135,* defines the distal boundary.

BAC cloning of the S-+ recombinant breakpoints encompassing the ''whipless'' defect. Prior to performing SSLP analysis on *S-+* recombinant Chr 17 homologs whose breakpoints fall within the *Pim*1 to *Crya*1 interval, a rudimentary partial physical map of that region was constructed by anchoring BAC contigs around four DNA markers in the region: *Pim1* and *Crya1,* markers flanking the originally defined *Hst6* locus (Pilder et al. 1993); *Tff3,* an intestinally expressed gene mapping centrally (17.0 cM) within the locus (Tomita et al. 1995; Chinery et al. 1996); and *H6.7b,* a member of a group of polymorphic DNA elements, formerly referred to as *Spretus-Hst6p* sequences (Redkar et al. 1998; see Materials and methods). Briefly, *Spretus-Hst6p* sequences are related DNA fragments mapped to the proximal portion of the *Hst6* locus by RFLP analysis. S^{r2}, S^{r6}, S^{r7}, and S^{r9} (none expressing the ''whipless'' trait when homozygous) carry + alleles of the *Spretus-Hst6p* sequences, while the remaining seven *S-+* recombinants (all expressing the ''whipless'' phenotype when homozygous) carry *s* alleles of the *Spretus-Hst6p* sequences (Figs. 2 and 3). A complete characterization of the *Spretus-Hst6p* sequences including *H6.7b* will be reported elsewhere (Fosella et al. in preparation).

After eliminating redundant BAC clones, the four contigs consist of 23 BACs, ranging in size from ~60 to ~210 kb. The library names of BAC clones making up the four contigs as well as informative STS markers generated by sequencing the BAC ends are listed in Table 2. In the text the BAC selected with an anchor marker is referred to as an A-BAC, BACs positioned proximally to the A-BAC are referred to as 1p, 2p, etc, with increasing numbers indicating greater distance from the A-BAC, and BACs positioned distally are referred to as 1d, 2d, etc, with increasing numbers indicating greater distance from the A-BAC. Each BAC name is prefaced by either a P-, C-, T-, or H- (abbreviations for the *Pim1, Crya1, Tff3,* or *H6.7b* contig, respectively).

Pim1 and Crya1 contigs: The *Pim1* contig, consisting of 8 adjacent BAC clones, has a minimum size of ~0.5 Mb and a maximum size of ~0.7 Mb as determined by inverse field gel analysis (data not shown). The P-A-BAC is followed distally by 3 BACs (P-1d through P-3d) and proximally by 4 BAC's (P-1p through P-4p) (Table 3). The orientation of the contig has been determined by content mapping of the following SSRs: *D17Mit167* (16.3 cM),

Table 2. BAC clones and sequences for BAC end STSs.

A	B	C	D	E	F	G
Pim1 contig						
P-A-BAC	613/H/23	165	5′-tcaaatgtcatctcctttcc-3′ 5′-accaaaaaccaaccaacc-3′	145	5′-ctctgacaggaatggtaac-3′ 5′-ctgtgctgtatgcacagac-3′	220
P-1p	203/J/18	125	5′-tggatgaagctcatcttcaaac-3′ 5′-ctcactgtctttcccatccc-3′	154	5′-tttgtgggttgaggagaaag-3′ 5′-cacagcagacagacagacagac-3′	277
P-2p	58/C/20	80	5′-tgccctgctatcaaccatc-3′ 5′-gttgttgttgttgttggag-3′	194	5′-atacccataactgtactccc-3′ 5′-gcagtgtcatcttattctcc-3′	253
P-3p	338/D/4	200	5′-actcgccagttctacatc-3′ 5′-gctcacaaccatctgtaag-3′	272	5′-accacagcctgctgaaagtc-3′ 5′-ggcagctagagatgagggaaac-3′	155
P-4p	569/G/21	130	*** ***		*** ***	
P-1d	393/F/19	170	5′-ccagagctaaagaatcaggtg-3′ 5′-cgttctctgtgtaatagccc-3′	155	cacatgcattctgagcttcc-3′ 5′-tgtgagcatagaaatccaccc-3′	196
P-2d	220/G/15	135	5′-gcaagcagacatttaaaagg-3′ 5′-atgggtcagggtttatgg-3′	108	5′-tcactcccaaaccacacgac-3′ 5′-ttcaggaccttcagaggacagc-3′	179
F-3d	188/G/13	70	5′-gcttttgttaagctgtcctc-3′ 5′-ggcctcagactttctgtaag-3′	241	5′-tggacaagctgatggatg-3′ 5′-agtctgtgctcttaactgctg-3′	261
Crya1 contig						
C-A-BAC	351/P/6	150	### ###		5′-ccagggaggaattggtagag-3′ 5′-ttgatggcagtctgcactc-3′	131
C-1p	37/1/12	200	5′-tgaggcagtcacatagtcag-3′ 5′-ctaagacaagtacctaacctaacc-3′	270	5′-cacacctcctaacccttccc-3′ 5′-cacaccctaacttctggtgc-3′	240
C-2p	371/M/4	140	### ###		5′-ttgcacactcatgcaacc-3′ 5′-aatgtagtcctccaaccctg-3′	160
C-3p	503/G/1	120	5′-ctgctttaactgtttgtgtc-3′ 5′-aagtctgttattggtccttg-3′	242	5′-atagggccagctccactaactg-3′ 5′-aagaggtggcttgctgaatg-3′	212
C-4p	571/E/24	75	*** ***		*** ***	
C-1d	51/J/6	200	5′-gaaggaagagagagatgggg-3′ 5′-ggaagtgatagggcacgaag-3′	299	5′-ggaagatagattgaaggtgac-3′ 5′-ggaactcaagttaaggttgtg-3′	149
C-2d	317/A/21	110	5′-tgacacacatttgaactctacc-3′ 5′-tcagacacaccagaagagg-3′	226	5′-cattgtctctgctcctgtg-3′ 5′-gggtcaggtagctgtaagtc-3′	149
C-3d	293/E/15	60	5′-gatcttctgctctacctccc-3′ 5′-ttgctaggaaaccgcatc-3′	262	5′-actcattttcccttcctgc-3′ 5′-gcttctgtgtgtgtgtgtttg-3′	202
Tff3 contig						
T-A-BAC	173/G/10	60	5′-tgacacaaaaccagccag-3′ 5′-tgacaggatgaaaatggtg-3′	203	5′-aaccactgtcagatgccaacc-3′ 5′-aaagttgtgtgccacctccg-3′	158
T-1p	283/H/8	95	### ###		5′-ccaaatatctttgaccaccc-3′ 5′-aggcagatggtacagatgg-3′	175
T-2p	138/O/17	130	5′-ccaagacagagtggttaggac-3′ 5′-tgccgtagaggaacatcag-3′	177	5′-tcttgacccttactccagcc-3′ 5′-acgttaaagctgcctgtcac-3′	188
T-1d	566/K/2	170	5′-gcatctcaagccacattc-3′ 5′-cattctaacctctccacagtc-3′	268	5′-tggactctggactctctctc-3′ 5′-cttgccttacagcatcac-3′	206
H6.7b contig						
H-A-BACa	582/O/5	110	5′-agcgaatctgacatcgtcc-3′ 5′-tgcagcacacacagcaaac-3′	229	5′-ggctatttctccagtatttc-3′ 5′-tgtaaatgtcgtctccttc-3′	216
H-A-BACb	272/E/23	175	5′-tagcccactaggaaaatg-3′ 5′-agcaagccagtaaggaac-3′	262	5′-gggatcatcaaaaggaggaag-3′ 5′-tcagacacagcagaagaggg-3′	181
H-A-BACc	324/M/10	210	5′-ccatccatcagcatatactgtc-3′ 5′-atgctcatagcctgccttc-3′	289	5′-gtcatagttttgagtgtcacc-3′ 5′-gctagaagctctcctttcc-3′	164

A = Contig/BAC
B = Library name
C = ~BAC size (kb)
D = SP6-end primers (forward/reverse)
E = STS size produced (bp)
F = T7-end primers (forward/reverse)
G = STS size produced (bp)
*** Not yet sequenced
Noninformative in contig extension.

D17Mit45, *D17Mit101*, *D17Mit228*, *D17Mit229* (16.4 cM), and *D17Mit60* and *D17Mit61* (16.8 cM) (Table 3; Fig. 2). P-4p carries *D17Mit167*, while P-2p carries *D17Mit45*. Since the intervening P-3p clone is ~200kb and contains neither SSR, the distance between these markers is at least 0.1 cM. Both the P-2p and P-1p clones contain *D17Mit101*, placing this marker less than 80 kb (the size of P-2p) from *D17Mit45*. Both the P-A-BAC and the P-1d clone carry *Pim1*, while no BAC in this contig contains *D17Mit228*, *D17Mit229*, *D17Mit60*, or *D17Mit61*. Since *Pim1* appears to be at the distal end of the P-A-BAC, *D17Mit101* cannot be more than 295 kb from *Pim1* (the total size of the P-A-BAC and P-1p combined), while *D17Mit228* and *D17Mit229* are distal to *Pim1* by more than 150 kb (the estimated minimal distance from the distal end of the P-A-BAC to the distal end of the P-3d clone.

The *Crya1*-anchored contig consists of eight adjacent BAC clones. The minimum size of this contig is ~0.4 Mb and its maximum size is ~0.6 Mb. As is the case with the *Pim1* contig, the anchor BAC, C-A-BAC, appears to be followed distally by 3 BACs (C-1d through C-3d) and proximally by 4 BAC's (C-1p through C-4p). The putative orientation of the contig has been determined by content mapping of the following SSRs: *D17Mit191* (17.2 cM), *D17Mit175* (17.7 cM), and *D17Mit63* (18.06 cM) (Table 3). Since neither *D17Mit191* nor *D17Mit63* is contained within the confines of the *Crya1* contig, the orientation of the contig is tentative, relying on the relative positions of *Crya1* and *D17Mit175*. Both of these latter markers are present on the C-A-BAC and the putative C-1d BAC. Thus, in the cell line CJ7 (Swiatek and Gridley 1993), a derivative of the mouse strain 129/Sv, from which the BAC library used here was constructed, *Crya1* (17.4 cM) and *D17Mit175* (17.7 cM) are not more than 150 kb

Table 3. SSR content of BAC contigs

Pim1 contig	*Mit167*	*Mit45*	*Mit101*	*Pim1*	*Mit228*	*Mit229*	*Mit60*	*Mit61*
P-A-BAC	–	–	–	+	–	–	–	–
P-1p	–	–	+	–	–	–	–	–
P-2p	–	+	+	–	–	–	–	–
P-3p	–	–	–	–	–	–	–	–
P-4p	+	–	–	–	–	–	–	–
P-1d	–	–	–	+	–	–	–	–
P-2d	–	–	–	–	–	–	–	–
P-3d	–	–	–	–	–	–	–	–
Crya1 contig	*Mit191*	*Crya1*	*Mit175*	*Mit63*				
C-A-BAC	–	+	+	–				
C-1p	–	–	–	–				
C-2p	–	–	–	–				
C-3p	–	–	–	–				
C-4p	–	–	–	–				
C-1d	–	+	+	–				
C-2d	–	–	–	–				
C-3d	–	–	–	–				
Tff3 contig	*Mit134*	*Mit199*	*Mit81*	*Mit135*	*Tff3*	*Mit146*	*Mit191*	
T-A-BAC	–	–	–	–	+	–	–	
T-1p	–	–	–	–	+	–	–	
T-2p	–	–	+	+	–	–	–	
T-1d	–	–	–	–	–	+	–	
H6,7b contig	*Mit61*	*H6.7b*	*Mit81*					
H-A-BACa	+	+	–					
H-A-BACb	+	+	–					
H-A-BACc	+	+	–					

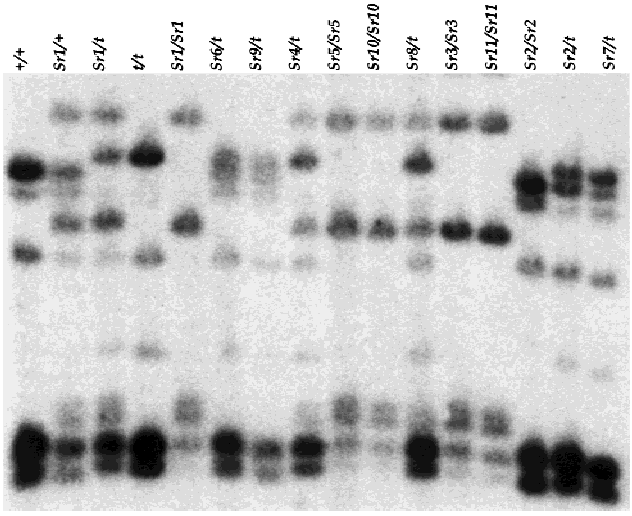

Fig. 3. Southern blot analysis of Taq I-digested DNAs extracted from tail tip biopsies of mice carrying either one or two copies of the eleven *S-+* recombinant Chr 17 homologs used in this study, and probed with radiolabeled *H6.7b*. Also included are DNA's extracted from +/+ and *t/t* controls. Genotypes are denoted above each lane. The *s* allele of *H6.7b* is seen in S^{r1}, S^{r3}, S^{r4}, S^{r5}, S^{r8}, S^{r10}, and S^{r11}-containing genomes, but not in S^{r2}, S^{r6}, S^{r7}, and S^{r9}-containing genomes. Mice homozygous for the *s* allele of *H6.7b* express ''whipless''.

apart, the approximate size of the C-A-BAC, the smaller of the two overlapping BACs carrying both markers. While we have not yet measured the relative distance of these two markers from the overlapping ends of either clone so that the chosen orientation of this contig is, at present, arbitrary, we do know that neither the *Pim1* nor the *Crya1* contig extends distally or proximally, respectively, far enough to incorporate the *S-+* breakpoints surrounding the gene(s) responsible for expression of the ''whipless'' defect.

The Tff3 contig. The *Tff3* contig consists of four adjacent BACs and has a minimum size of ~0.35 Mb and a maximum size of ~0.45 Mb. The T-A-BAC is preceded proximally by 2 BAC's (T-1p and T-2p), and is followed distally by 1 BAC (T-1d). The orientation of the contig has been determined by content mapping of the following SSRs: *D17Mit81, D17Mit134, D17Mit199* (16.9 cM), *D17Mit135* (17.0 cM), *D17Mit146* (17.1 cM), and *D17Mit191* (17.2 cM) (Table 3). Both the T-A-BAC and the T-1p clone overlap at *Tff3* (17.0 cM), while neither carries any of the seven tested SSRs. However, the T-2p clone carries both *D17Mit81* and *D17Mit135*, and the T-1d BAC contains *D17Mit146*. None of the other tested SSRs are carried by the members of this small contig. These data indicate that *D17Mit81* and *D17Mit135* are within 135 kb of each other (the size of the T-2p BAC), and that *Tff3* is less than 230 kb from either of these two markers (the total size of T-1p and T-2p, if their individual sizes are added together). Thus, the distal breakpoint of the *Hst6* locus-specific ''whipless'' phenotype (defined by the proximal *S-+* recombinant breakpoint of S^{r2}) resides between *D17Mit81* and *D17Mit135* on the T-2p BAC, less than 230 kb proximal to *Tff3* (Fig. 2). Additionally, *Tff3* must be proximal to *D17Mit146* by less than 235 kb (the total size of the T-A-BAC and T-1d, if their individual sizes are added together). Although other SSRs tested do not appear to be contained within this contig, a probable marker order, based on this work and previously published data (Hamvas et al. 1998; Heine et al. 1998), would be [*D17Mit134, D17Mit199*]–*D17Mit81*–''whipless''/*Ccua* distal breakpoint–*D17Mit135*–*Tff3*–*D17Mit146*–*D17Mit191*.

The H6.7b contig. The *H6.7b* contig is the smallest of the four contigs, consisting of three overlapping, but highly informative BACs. The total size of the contig is ~210 kb and consists of three anchor clones, hereafter referred to as H-A-BACa, H-A-BACb, and H-A-BACc, with the largest, H-A-BACc, totally encompassing the other two. The individual sizes are, thus, ~210 kb for H-A-BACc, ~175 kb for H-A-BACb, and ~110 kb for H-A-BACa. All three carry *H6.7b*, and all three have been tested for SSR content, using *D17Mit61* (16.8 cM) and *D17Mit81* (16.9 cM). While none carries *D17Mit81*, all three contain *D17Mit61* (Table 3; Fig. 2). Recalling that the recombinant Chr 17 homolog S^{r6} carries the *s* allele of *D17Mit61* but the + allele of *H6.7b*, the

proximal breakpoint of the *Hst6* locus-specific ''whipless'' phenotype (defined by the distal S-+ recombinant breakpoint of S^{r6}) resides between *D17Mit61* and *H6.7b*, which are less than 110 kb from each other on H-A-BACa (Fig. 2).

In summary, based on the analyses of all Chr 17 homologs and BAC contigs from this study, a probable marker order of all markers used here is *D17Mit167–D17Mit45–D17Mit101–Pim1–*[*D17Mit228, D17Mit229, D17Mit60–D17Mit61*]*–H6.7b–*[*D17Mit134, D17Mit199*]*–D17Mit81–D17Mit35–Tff3–D17Mit146–D17Mit191–* [*Crya1, D17Mit175*]*–D17Mit63–D17Leh89*, with the order of bracketed markers being uncertain. While this is in good agreement with previous linkage studies (Dietrich et al. 1996; Heine et al. 1998), markers previously shown to map to the identical genetic position (for example, *D17Mit45, D17Mit101, Pim1, D17Mit228,* and *D17Mit229*) are here separated from each other and ordered along a proximal to distal axis (although the relative order of *D17Mit228* and *D17Mit229* remains unknown, as indicated above). Still other markers are shown to be much closer together than previously indicated (*Crya1* and *D17Mit175*).

Discussion

The *Hst6* locus was originally mapped on mouse Chr 17 in the *Pim1* to *Crya1* interval, a genetic map distance of ~1 cM (Pilder et al. 1993). $Hst6^s/t$ males were shown to be sterile and produced sperm that displayed an associated trait called ''curlicue'', a chronic flagellar curvature phenotype. $Hst6^s/Hst6^s$ males proved also to be sterile, but this was due to the fact that the sperm produced by these animals were lacking assembled axonemes, the functional backbones of sperm tails (Pilder et al. 1993; Phillips et al. 1993; this phenotype is now officially named ''whipless''). Initially, it was proposed that *Hst6* might be a candidate locus for the powerful *t*-distorter/sterility factor *Tcd/Tcs2,* and that the two distinct *Hst6*-specific phenotypes (''curlicue'' and ''whipless'') could both be explained by the interaction of alleles of a single gene, a loss of function *s* allele and an altered function *t* allele (Pilder et al. 1993). However, recent evidence has shown that at least two factors are responsible for the quantitative expression of the ''curlicue'' phenotype, *Ccua*, located proximally in the *Hst6* locus, and *Ccub*, located distally (Redkar et al. 1998). Thus, the growing phenotypic complexity of the *Hst6* locus prompted a reappraisal of *Hst6* genetics with particular emphasis upon the relationship, if any, of ''whipless'' to the Curlicue factors.

The data reported here show that the ''whipless'' phenotype is expressed in sperm from males homozygous for *M. spretus* chromatin distal to the S^{r6} distal recombinant breakpoint and proximal to the S^{r2} proximal breakpoint. This region is identical to the *Ccua* locus (Redkar et al. 1998), implying that a single gene hypothesis is still sufficient to explain both the total expression of the ''whipless'' phenotype and a partial expression of the ''curlicue'' phenotype. However, the relationships between *s* and *t* alleles of *Ccub* and between *Ccub* and *Ccua* may be more complicated. While $Ccua^+$ $Ccub^s/t$ males are sterile, homozygosity for $Ccub^s$ alone produces neither observable sperm morphological defects, apparent motility deficits, nor male sterility. The simplest explanation of these findings is that $Ccub^s$ is recessive and allelically hypostatic to $Ccub^t$. However, since the *t* alleles of both *Ccua* and *Ccub* cannot be separated from each other, it is just as likely that the expression of $Ccub^s$ is influenced by $Ccua^t$ or the combination of $Ccua^t$ and $Ccub^t$ in the $Ccua^+Ccub^s/t$ heterozygote. It is also noteworthy that *Stop1p*, a factor putatively involved in sperm-oolemma penetration (Redkar et al. 1998), is flanked by the Curlicue loci. While *Stop1p* activity probably has no effect on sperm tail assembly or function, its contribution to the sterility phenotype of $Ccua^sStop1p^sCcub^+/t$ and/or $Ccua^+Stop1p^sCcub^s/t$ males could be significant. Thus, at present, *Hst6* (and possibly by analogy, *Tcd/Tcs2*) seems substantially more complex than previously envisioned, containing a genetically complicated network of elements whose gross impact upon sperm differentiation and function can be devastating.

An improved understanding of the relationships between the various aforementioned *Hst6*-specific factors will require their eventual positional cloning and molecular analysis. To that end, we have established an aggregate high-resolution genetic and partial physical map of the *Pim1* to *Crya1* interval (Fig. 2), using SSLP analysis of phenotypically relevant *S-+* recombinant Chr 17 homologs, and SSR content mapping of four BAC contigs anchored by well-spaced markers in the region. This simple approach not only allows for the ordering of and determination of physical distances between closely spaced markers, but their relationships to each other along the proximal to distal chromosomal axis. In addition, BAC end sequencing has provided us with a series of new STS markers, some of which may prove to be informative in establishing the physical position of locus-specific recombinant breakpoints and in cloning candidate genes for the various *Hst6*-specific traits.

Except for producing a marker order for and maximal physical distances between several SSR's that had been genetically mapped to an identical location, the *Pim1* BAC contig, with its distal extent ~0.3–0.4 cM proximal to *Ccua,* has been the least informative of all of the contigs yet isolated. Additionally, the *Crya1* contig has not yet provided highly informative data with respect to the distal limit of the *Ccub* locus, because its directionality has not yet been convincingly established. Only three SSRs were used in *Crya1* contig content mapping, and only one, *D17Mit175,* mapped to the contig. Because the experimentally determined physical distance of *D17Mit175* from the anchor marker, *Crya1,* was significantly less than would be expected from the genetic distance reported in several studies (Hamvas et al. 1998; Heine et al. 1998), *D17Mit175* was not highly informative in establishing the proximal and distal ends of the contig. However, SSLP analysis of S^{r7} has established that the *Ccub* distal limit is distal to *D17Mit191* but proximal to the S^{r7} proximal recombinant breakpoint (Fig. 2). Further analysis of S^{r7} and S^{r8} with polymorphic STSs derived via *Crya1* contig-BAC end sequencing may be helpful in establishing the directionality of this contig and the position of the *Ccub* distal limit.

The map drawn from these experiments does clearly define the genetic sizes of the ''whipless''/*Ccua*, *Stop1p,* and *Ccub* loci as <0.2 cM, <0.3 cM and <0.3 cM, respectively (distal to 16.8–proximal to 17.0 cM for *Ccua,* distal to 16.9–proximal to 17.2 cM for *Stop1p,* and distal to 17.1–proximal to 17.4 cM for *Ccub;* Table 1). In addition, three recombinant breakpoints for the two most proximal loci, *Ccua* and *Stop1p,* have been cloned in two BAC's. The T-2pBAC is the site of the proximal recombinant breakpoint offsetting the *Stop1p* locus. Although the *Stop1p* distal/*Ccub* proximal breakpoint has not yet been isolated, roughly the proximal two-thirds of the *Stop1p* locus has been cloned in the form of the *Tff3* BAC contig, and a maximum physical size of this ~0.2 cM region has been established as ~465 kb. The presence of *Tff3* within the *Stop1p* locus makes it a candidate for *Stop1p* by position. However, while the putative role of *Tff3* in epithelial cell adhesion (Efstathiou et al. 1998) is intriguing in terms of possible *Stop1p* function, there is absolutely no evidence that *Tff3* is expressed either in the normal or mutant male genital tract or is present in sperm. Thus, its candidacy for *Stop1p* remains highly doubtful.

The distal recombinant breakpoint of the *Ccua* locus is identical to the proximal recombinant breakpoint offsetting the *Stop1p* locus, and is thus carried by the T-2pBAC. The proximal breakpoint for *Ccua* has also been isolated in a single small BAC clone, H-A-BACa. While the total size of the *Ccua* locus is not yet known, its genetic distal half is physically less than 135 kb (the size of the T-2pBAC, which carries both *D17Mit135* distally and *D17Mit81* proximally). If significant clustering of SSR's in the

Ccua locus is the case as has been previously reported for other loci (Arveiler and Porteous 1992; Fukagawa et al. 1995; Gregorova et al. 1996), the physical distance between *D17Mit61* (16.8 cM) and *D17Mit81* (16.9 cM) may be small. Thus, the isolation of the *Ccua* recombinant breakpoints, the potential small size of this locus, and the cloning of additional polymorphic markers internal to this region (*Spretus-Hst6p* sequences; see Materials and methods) make it an ideal candidate for further physical dissection.

Acknowledgments. The authors would like to thank Professor Trish Olds-Clarke for help in preparing and videotaping sperm samples. This work was supported by National Institutes of Health Grant HD31164 and National Science Foundation Grant 9513464 to S.H.Pilder.

References

Arveiler B, Porteous DJ (1992) Distribution of Alu and L1 repeats in human YAC recombinants. Mamm Genome 3, 661–668

Chinery R, Poulsom R, Cox HM (1996) The gene encoding mouse intestinal trefoil: structural organization, partial sequence analysis, and mapping to murine Chromosome 17q. Gene 171, 249–253

Dietrich WF, Miller JC, Steen RG, Merchant MA, Damron-Boles D, et al. (1996) A comprehensive genetic map to the mouse genome. Nature 380, 149–154

Efstathiou JA, Noda M, Rowan A, Dixon C, Chinery R, et al. (1998) Intestinal trefoil factor controls the expression of the adenomatous polyposis coli-catenin and the E-cadherin-catenin complexes in human colon carcinoma cells. Proc Natl Acad Sci USA 95, 3122–3127

Fukagawa T, Sugaya K, Matsumoto K, Okumura K, Ando A, et al. (1995) A boundary of long-range G+C% mosaic domains in the human MHC locus: pseudoautosomal boundary-like sequence exists near the boundary. Genomics 25, 184–191

Gregorova S, Mnukova-Fajdelova M, Trachtulec Z, Capkova J, Loudova M, et al. (1996) Sub-milliMorgan map of the proximal part of mouse Chromosome 17 including the hybrid sterility 1 gene. Mamm Genome 7, 107–113

Hammer MF, Schimenti J, Silver LM (1989) Evolution of mouse chromosome 17 and the origin of inversions associated with *t* haplotypes. Proc Natl Acad Sci USA 86, 3261–3265

Hamvas RMJ, Trachtulec Z, Vernet C, Forejt J (1998) Mouse Chromosome 17. Mamm Genome 8(Suppl), S320–S342

Heine D, Khambata S, Passmore HC (1998) High-resolution and recombination interval analysis of mouse Chromosome 17. Mamm Genome 9, 511–516

Lyon MF (1984) Transmission ratio distortion in mouse *t* haplotypes is due to multiple distorter genes acting on a responder locus. Cell 37, 621–628

Lyon MF (1986) Male sterility of the mouse *t* complex is due to homozygosity of the distorter genes. Cell 44, 357–363

Neill JM, Olds-Clarke P (1987) A computer-assisted assay for mouse sperm hyperactivation demonstrates that bicarbonate but not bovine serum albumin is required. Gamete Res 18, 121–140

Olds-Clarke P, Johnson LR (1993) *t* Haplotypes in the mouse compromise sperm flagellar function. Dev Biol 155, 14–25

Phillips DM, Pilder SH, Olds-Clarke P, Silver LM (1993) Factors that may regulate assembly of the mammalian sperm tail deduced from a mouse *t* complex mutation. Biol Reprod 49, 1347–1352

Pilder SH (1997) Identification and linkage mapping of *Hst7,* a new *M. spretus/M. m. domesticus* chromosome 17 hybrid sterility locus. Mamm Genome 8, 290–291

Pilder SH, Hammer M, Silver LM (1991) A novel mouse chromosome 17 hybrid sterility locus: implications for the origin of *t* haplotypes. Genetics 129, 237–246

Pilder SH, Olds-Clarke P, Phillips DM, Silver LM (1993) *Hybrid Sterility 6:* a mouse *t* complex locus controlling sperm flagellar assembly and movement. Dev Biol 159, 631–642

Pilder SH, Olds-Clarke P, Orth JM, Jester WF, Dugan L (1997) *Hst7:* a male sterility mutation perturbing sperm motility, flagellar assembly, and mitochondrial sheath differentiation. J Androl 18, 663–671

Redkar AA, Olds-Clarke P, Dugan LM, Pilder SH (1998) High-resolution mapping of sperm function defects in the *t* complex fourth inversion. Mamm Genome 9, 825–830

Swiatek PJ, Gridley T (1993) Perinatal lethality and defects in hindbrain development in mice homozygous for a targeted mutation of the zinc finger gene *Krox 20.* Genes & Dev 7, 2071–2084

Tomita M, Itoh H, Ishikawa N, Higa A, Ide H, et al. (1995) Molecular cloning of mouse intestinal trefoil factor and its expression during goblet cell changes. Biochem J 311, 293–297